VILNIUS TECH
Vilnius Gediminas Technical University

Proceedings of the 13th International Scientific Conference

ENVIRONMENTAL ENGINEERING

April 23–24, 2026, Vilnius, LITHUANIA

eISSN 2029-7092
eISBN 978-609-476-444-8
Article ID: enviro.2026.2360
https://doi.org/10.3846/enviro.2026.2360

III. GEOSPATIAL TECHNOLOGIES AND INNOVATIONS IN GEODESY, REMOTE SENSING, AND ENVIRONMENTAL MONITORING

http://vilniustech.lt/enviro

UAV-BASED ROCK MASS CHARACTERIZATION FOR GEOLOGICAL STRENGTH INDEX (GSI) ASSESSMENT AND COMPARISON WITH CONVENTIONAL FIELD MAPPING

Ahmad Zharfan Ahmad HUSAINI[1], Vynotdni RATHINASAMY[1*], Mohamad Syazwan Mohd ROSLEE[1], Mohd Ashraf Mohamad ISMAIL[1], Ramesh Murlidhar BHATAWDEKAR[2], Dayang Zulaika Abang HASBOLLAH[2], Eka Kusmawati SUPARMANTO[3], Luo JIALIANG[1]

[1]*School of Civil Engineering, Universiti Sains Malaysia, Nibong Tebal, 14300 Pulau Pinang, Malaysia*
[2]*Centre of Tropical Geoengineering, Universiti Teknologi Malaysia, Johor Bahru, 81310 Johor, Malaysia*
[3]*Geotechnical Engineering Branch, Public Works Department of Malaysia (JKR), 50400 Selangor, Malaysia*

Received 23 January 2026; revised 4 March 2026; accepted 5 March 2026

Abstract. Rock mass characterization is essential for reliable Geological Strength Index (GSI) estimation, particularly in inaccessible or steep slopes where conventional field mapping is challenging. This study evaluates the feasibility of utilizing Unmanned Aerial Vehicle (UAV)-based photogrammetry for GSI assessment using the Cai et al. (2004) chart in a granitic outcrop in Machang, Kelantan, Malaysia. Quantitative parameters, including block volume (Vb) and joint roughness, were derived from 3D point clouds, while joint condition factors (Jc) were assessed through both manual and UAV approaches. Results show strong correlation between UAV and manual assessments (R^2 = 0.9894 for GSI). The findings demonstrate that UAV-based methods can reliably replace conventional field mapping, improving safety, efficiency, and data density for GSI assessment of Cai et al. (2004).

Keywords: UAV, Geological Strength Index (GSI), rock mass characterization.

1. Introduction

Rock mass characterization is a major element of geological engineering especially when dealing with excavations and natural slopes (Siddique, 2024). This assessment has to be carefully carried out to ensure proper design of tunnels and quarries as failures certainly lead to major safety hazards and economic loss (Benfield, 2023). Many researchers have dependent on manual field mapping for discontinuity survey and surface condition observations. Yet, in the areas with unaccesable or steep slopes, this traditional method becomes a challege in the field. Over the years, remote sensing has been integrated into field mapping (Zafaty et al., 2023; Zamzam, 2023). The Unmanned Aerial Vehicles (UAV) has aided in photographing and developing high-resolution 3D point clouds which allow users to analyze the outcrops remotely.

Geological Strength Index (GSI) is one of the prominent rock mass classification system as it could be directly correlated with Hoek-Brown rock mass failure criterion (Pozo, 2022a). Although this system fundamentally dependent on visual characterisation, in recent years many researchers (Morelli, 2015; Pozo, 2022b; Saptono & Rezky, 2023) have integrated quantified measurements for the assessment. This includes incorporation of Rock Quality Designation (RQD), volumetric count joint and block volume (Cai et al., 2007; Russo, 2009; Xia et al., 2022). However, the GSI requires sophisticated data collection which requires more labour work and duration for fieldwork.

The UAV has been applied in large context for rock mass characterization including discontinuity survey, RQD system, Q-system, surface roughness and Rock Mass Rating (RMR). However, the utilization of UAV for GSI classification is still limited. Several researchers have started exploring this in recent years (Benfield, 2023; Ge et al., 2023; Moomivand et al., 2026). In line with that, this study aims to evaluate the feasibility of using UAV for GSI assessment of Cai et al. (2004). This particular GSI chart incorporates both quantitative (joint roughness, block volume) and qualitative (joint condition) measurement. Thus, the study can evaluate the feasibility for both type of measurements.

* Corresponding author. E-mail: *vynotdni@usm.my*

2. Geology of study area

Machang is a city located in northeast state of Peninsular Malaysia which is Kelantan. The area is underlain mainly by Permian phyllite, slate, shale, limestone and widespread volcanic rock. During the study, the study area was found to be intruded by granite with minor granodiorite. The outcrop exhibited well developed blocky structure with moderately to highly weathered rock mass as in Figure 1.

Figure 1. Site location and geology map of the area (modified from Arifin et al., 2019)

3. Methodology

The GSI chart of Cai et al. (2004) has block volume (Vb) as its y-axis and joint condition (Jc) factor as x-axis. The block volume is calculated using Eq. (1).

$$Vb = s1s2s3 / \sin\gamma_1 \sin\gamma_2 \sin\gamma_3 , \quad (1)$$

where, s is joint spacing while γ is angle between joint set. Whereas, the Jc is caluclated using Eq. (2).

$$Jc = JwJs / Ja, \quad (2)$$

where, Jw is large-scale waviness, Js is small-scale smoothness while Ja is joint alteration. Parameters such as joint spacing, angle between joint and waviness require quantitative measurement from outcrop. However, the joint smoothness and alteration only require visual observation from outcrop. These observation are then rated based on Cai et al. (2004) rating systems. As previously mentioned, this study aims to utilize the UAV for GSI assessment of Cai et al. (2004). Additionally, the study evaluates the difference between manual and UAV assessments for the Jc parameters only. Therefore, the parameters for Vb were assessed through UAV only.

Due to the massive size of outcrop, it was divided into 3 panels for the assessment and the orientation of joint sets were measured using Barton compass. Then, the photogrammetry began by deploying a UAV to capture high-resolution imagery of the entire outcrop. These images were processed to generate a 3D point cloud. DroneDeploy software was utilised to measure the joint spacings directly from the digital model. This remote sensing approach enhances the safety by eliminating the need for manual climbing and allows for efficient data extraction in a laboratory setting. The point cloud was the imported into CloudCompare to determine the orientation, specifically strike and dip angle. Understanding these orientations is critical for predicting how the rock mass behaves under stress. Similarly, ShapeMetriX was employed to analyse the point cloud data to determine the roughness of joint sets. While the manual approach utilised a Barton comb for waviness measurement by panel, the UAV approach allowed for a significantly higher density of measurements. This digital method provides a detailed roughness profile. It enables the rapid extraction of amplitudes and distance values. As a result, the UAV-based method increases workflow efficiency and data volume while reducing field exposure time.

4. Results

As the outcrop was divided into 3 panels (Figure 2), each of it was assesses individually. First the discontinuity survey was carried out. All the panels had 3 joint sets. The orientation of joint sets are tabulated in Table 1. The Joint set 1 to 4 are almost in the same orientation except for Joint 5.

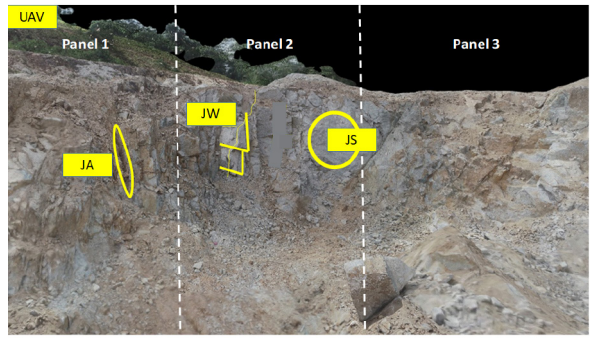

Figure 2. Outcrop divided into 3 panels for assessment

Table 1. Orientation of joint sets

Joint	Number of joints	Strike	Dip angle
1	17	266	75
2	10	230	36
3	23	276	74
4	24	251	61
5	16	175	59

4.1. Block Volume (Vb)

The Vb is calculated using joint spacing and angle between them. Table 2 shows the measurement of these parameters which were obtained from UAV assessent. The Joint set 5 has the shortest joint spacing of 35 cm while Joint set 1 has the longest spacing of 93 cm. This certainly reflects the heterogeneous nature of rock mass fracture

system. In GSI assessment, the joint spacing is the main influencing factor (Singh et al., 2023). The joints in general are weak planes of rock. Thus, the fractured area lowers overall strength of rockmass which directly alters the value of GSI (Ghorbani et al., 2025).

Table 2. Joint spacing (s) and angle between them (γ)

Joint	Average joint spacing (s)	Average angle between joints (γ) (°)
1	93	103
2	61	117
3	49	90
4	51	90
5	35	123

Based on the values in Table 2, the Vb was calculated for each panel. The Vb for Panel 1 is 565783 cm^3, Panel 2 is 1746652 cm^3 while Panel 3 is 1876108 cm^3.

4.2. Joint Condition Factor (Jc)

As compared to Vb, the assessment of Jc requires more time in the field. There are 3 parameters studied for this Jc such as large-scale waviness, small-scale smoohness and joint alteration. All these parameters were carried out manually and using UAV. Table 3 summarises the findings of the parameters as well as calculated Jc values.

Table 3. Findings for Jc parameters

Panels	Manual				UAV			
	Ja	Jw	Js	Jc	Ja	Jw	Js	Jc
Panel 1	2	1	2	1	2	1	2	1
Panel 2	1	1	3	3	1	1	3	3
Panel 3	2	1	2	1	2	1	2	1

Based on the observation, both the Panel 1 and 3 are nearly flat with rough joint surface and one grade higher infiilings. Whereas, the Panel 2 is nealy flat with very rough interlocking joint planes and no infilling.

Figures 3–6 show the correlation between manual measurement/observation with UAV utilization for Ja, Jw, Js and Jc respectively. All the correlation coefficient, R^2 shows strong linear correlation of 1. It must be noted that two parameters of Jc are related to visual observation. Thus, this relation shows that the visual observation of joint alteration and smoothness are similar to observation in UAV. Ge et al. (2023) who utilised UAV for GSI of Marinos and Hoek (2000) also found that UAV observation for surface conditions is amost similar to manual observation. It must be noted that Ja is a important factor which reflects the weather and infilling (Ge et al., 2023). On the other hand, there is a slight variation (R^2 = 0.9348) in undulation between manual and UAV as in Figure 7. Yet, when the values are rated according to Cai et al. (2004), the Jw rating is found to be 1 for both UAV and manual methods as in Figure 4. Many studies (Salvini et al., 2020; Adnan et al., 2023) have been done on utilization of UAV for surface roughness which also suggest good correlation of manual and UAV results.

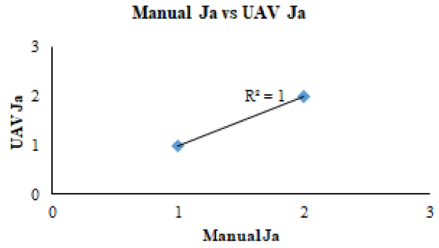

Figure 3. Manual Ja versus UAV Ja

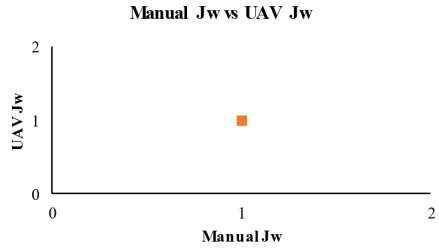

Figure 4. Manual Jw versus UAV Jw

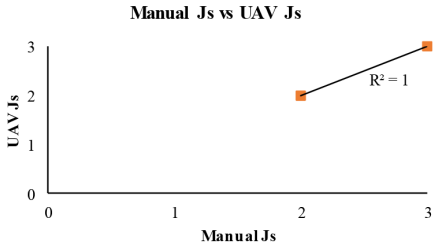

Figure 5. Manual Js versus UAV Js

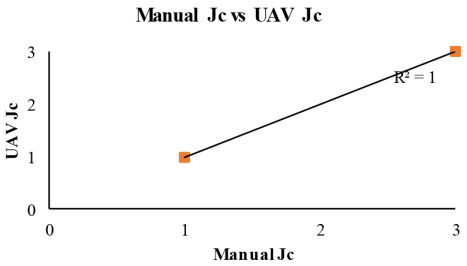

Figure 6. Manual Jc versus UAV Jc

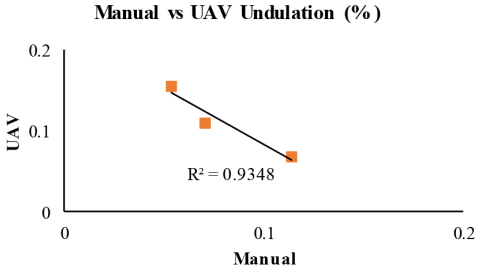

Figure 7. Manual versus UAV undulation (%)

4.3. Geological Strength Index (GSI)

Based on the measurements and calculations above, the GSI value is calculated and plotted in Cai t al. (2004) chart as in Figure 8. The manual GSI values for Panel 1 is 66, Panel 2 is 82 and Panel 3 is 70 respectively. Meanwhile, the UAV utilized GSI values for Panel 1 is 65, Panel 2 is 82 and Panel 3 is 70 respectively. Figure 9 shows the correlation between both type GSI values which is R2 of 0.9894. This indicates a strong correlation and encourages utilization of UAV for GSI assessment.

5. Discussion and conclusions

The study utilizes paneling of outcrop to ensure better GSI estimation similar to Ge et al. (2023). Partitioning the rock mass is good for estimation especially in tropical regions where differential weathering is common. Although this study lacks in terms of number of datasets, the difference in surface condition is still vivid as Panel 2 which is situated in the middle has slightly different Jc. Partitioning in manual GSI work is time consuming and labour intensive especially when utilizing GSI of Cai et al. (2004).

It must be also noted that all the parameters in GSI chart of Cai et al. (2004) which were measured using UAV are strongly correlated (R^2 of 1) with manual calculation and observation.

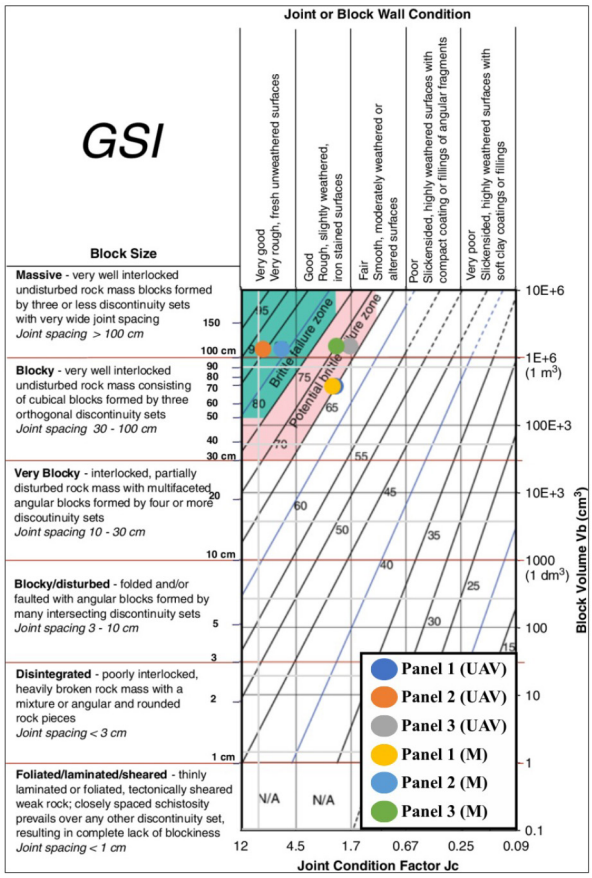

Figure 8. GSI values for both UAV and manual calculation

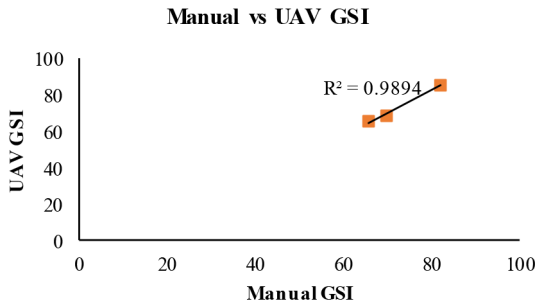

Figure 9. Manual GSI versus UAV GSI

Other studies which utilized UAV partially for other GSI charts also proved that the photogrammetry technique is as good as manual observation (Farmakis et al., 2019; Ge et al., 2023; Moomivand et al., 2026). Therefore, this study shows UAV shall be utilised fully for all parameters for GSI chart of Cai et al. (2004).

Acknowledgements

The publication was fully supported by Ministry of Higher Education of Malaysia through FRGS/1/2023/TK01/USM/02/1.

References

Adnan, R. A. A. R., Ismail, M. A. M., Tobe, H., Miyoshi, T., Date, K., & Yokota, Y. (2023). Preliminary assessment of joint roughness coefficient of rock slope using UAV–SfM photogrammetry technique. *Journal of the Geological Society of India*, *99*(10), 1465–1473. https://doi.org/10.1007/s12594-023-2493-8

Arifin, M. H., Kayode, J. S., Izwan, M. K., Zaid, H. A. H., & Hussin, H. (2019). Data for the potential gold mineralization mapping with the applications of Electrical Resistivity Imaging and Induced Polarization geophysical surveys. *Data in Brief*, *22*, 830–835. https://doi.org/10.1016/j.dib.2018.12.086

Benfield, S. L. (2023). *Site characterization using drone based photogrammetry* [Master's thesis, Colorado School of Mines]. https://repository.mines.edu/bitstreams/24dbf407-9db9-43d7-b278-a3d8b75b3d82/download

Cai, M., Kaiser, P. K., Uno, H., Tasaka, Y., & Minami, M. (2004). Estimation of rock mass deformation modulus and strength of jointed hard rock masses using the GSI system. *International Journal of Rock Mechanics and Mining Sciences*, *41*(1), 3–19. https://doi.org/10.1016/S1365-1609(03)00025-X

Cai, M., Kaiser, P. K., Tasaka, Y., & Minami, M. (2007). Determination of residual strength parameters of jointed rock masses using the GSI system. *International Journal of Rock Mechanics and Mining Sciences*, *44*(2), 247–265. https://doi.org/10.1016/j.ijrmms.2006.07.005

Ge, Y., Chen, Q., Tang, H., Cao, B., & Hussain, W. (2023). A Semi-automatic approach to quantifying the geological strength index using terrestrial laser scanning. *Rock Mechanics and Rock Engineering*, *56*(9), 6559–6579. https://doi.org/10.1007/s00603-023-03412-1

Ghorbani, E., Shahinfar, M., & Taheri, A. (2025). A review of the geological characterization, classification, modeling, and

case studies of anisotropic rock masses. *Deep Resources Engineering*, *2*(4), Article 100219. https://doi.org/10.1016/j.deepre.2025.100219

Farmakis, I., Marinos, V., & Vlachopoulos, N. (2019, June 23–26). Assessment of the GSI along rock slopes based on LiDAR and photogrammetry point clouds. In *Proceedings of the 53rd U.S. Rock Mechanics/Geomechanics Symposium* (ARMA-2019-2057). New York City, New York.

Moomivand, H., Soltanalinejad, S., & Allahverdizadeh, H. (2026). Development of a new method for evaluating the geological strength index (GSI) by applying image analysis to in-situ rock mass. *Bulletin of Engineering Geology and the Environment*, *85*, Article 158. https://doi.org/10.1007/s10064-026-04778-6

Morelli, G. L. (2015). Variability of the GSI index estimated from different quantitative methods. *Geotechnical and Geological Engineering*, *33*, 983–995. https://doi.org/10.1007/s10706-015-9880-x

Pozo, R. (2022a). Equivalent Geological Strength Index (GSI) approach with application to rock mass slope stability. *Rudarsko-geološko-naftni zbornik*, *37*(4), 53–70. https://doi.org/10.17794/rgn.2022.4.5

Pozo, R. (2022b). Comparative analysis of different calculation methods of the Geological Strength Index (GSI) based on qualitative and quantitative approaches. *Rudarsko-geološko-naftni zbornik*, *37*(3), 121–138. https://doi.org/10.17794/rgn.2022.3.10

Russo, G. (2009). A new rational method for calculating the GSI. *Tunnelling and Underground Space Technology*, *24*(1), 103–111. https://doi.org/10.1016/j.tust.2008.03.002

Salvini, R., Vanneschi, C., Coggan, J. S., & Mastrorocco, G. (2020). Evaluation of the use of UAV photogrammetry for rock discontinuity roughness characterization. *Rock Mechanics and Rock Engineering*, *53*, 3699–3720. https://doi.org/10.1007/s00603-020-02130-2

Saptono, S., & Rezky, D. M. (2023). Application Geological Strength Index (GSI) quantification method on the characterization of carbonate rock mass. *Journal of Sustainable Mining*, *22*(3), Article 5. https://doi.org/10.46873/2300-3960.1387

Siddique, T. (2024). Rock mass classification in slope engineering with special emphasis on Slope mass rating: Current status and future projections. *Geological Journal*, *59*(9), 2472–2486. https://doi.org/10.1002/gj.4933

Singh, J., Pradhan, S. P., Vishal, V., & Singh, M. (2023). Characterization of a fractured rock mass using geological strength index: A discrete fracture network approach. *Transportation Geotechnics*, *40*, Article 100984. https://doi.org/10.1016/j.trgeo.2023.100984

Zafaty, O., Oukassou, M., Mhamdi, H. S., Tabuce, R., & Chariere, A. (2023). Integrated remote sensing data and field investigations for geological mapping and structural analysis. The case of SW Tichoukt ridge (Middle Atlas, Morocco). *Journal of African Earth Sciences*, *198*, Article 104784. https://doi.org/10.1016/j.jafrearsci.2022.104784

Xia, K., Chen, C., Wang, T., Pang, H. & (2022). Quantification of the GSI and D values in the Hoek–Brown criterion using the rock quality designation (RQD) and discontinuity surface condition rating (SCR). *Bulletin of Engineering Geology and the Environment*, *81*, Article 4. https://doi.org/10.1007/s10064-021-02493-y

Zamzam, S. (2023). Geological controls and prospectivity mapping for manganese ore deposits using predictive modeling comparison: An integration of outcrop and remote sensing data, Sinai microplate, Egypt. *Journal of Earth Science*, *34*, 588–608. https://doi.org/10.1007/s12583-021-1583-z